(12) INTERNATIONAL APPLICATION PUBLISHED UNDER THE PATENT COOPERATION TREATY (PCT)

(19) World Intellectual Property Organization
International Bureau

(43) International Publication Date
10 December 2015 (10.12.2015)

WIPO | PCT

(10) International Publication Number
WO 2015/187489 A1

(51) International Patent Classification:
A61B 5/00 (2006.01)

(21) International Application Number:
PCT/US2015/033229

(22) International Filing Date:
29 May 2015 (29.05.2015)

(25) Filing Language: English

(26) Publication Language: English

(30) Priority Data:
62/007,891 4 June 2014 (04.06.2014) US

(71) Applicant: **UNIVERSITY OF MASSACHUSETTS MEDICAL SCHOOL** [US/US]; 225 Franklin Street, 12th Floor, Boston, MA 02100 (US).

(72) Inventor: **CHIN, Michael, S.**; 31 Pointe Rok Drive, Worcester, MA 01604 (US).

(74) Agent: **ZHANG, Yin, Philip**; Milstein Zhang & Wu LLC, 2000 Commonwealth Ave. Suite 400, Newton, MA 02466 (US).

(81) Designated States *(unless otherwise indicated, for every kind of national protection available)*: AE, AG, AL, AM, AO, AT, AU, AZ, BA, BB, BG, BH, BN, BR, BW, BY, BZ, CA, CH, CL, CN, CO, CR, CU, CZ, DE, DK, DM, DO, DZ, EC, EE, EG, ES, FI, GB, GD, GE, GH, GM, GT, HN, HR, HU, ID, IL, IN, IR, IS, JP, KE, KG, KN, KP, KR, KZ, LA, LC, LK, LR, LS, LU, LY, MA, MD, ME, MG, MK, MN, MW, MX, MY, MZ, NA, NG, NI, NO, NZ, OM, PA, PE, PG, PH, PL, PT, QA, RO, RS, RU, RW, SA, SC, SD, SE, SG, SK, SL, SM, ST, SV, SY, TH, TJ, TM, TN, TR, TT, TZ, UA, UG, US, UZ, VC, VN, ZA, ZM, ZW.

(84) Designated States *(unless otherwise indicated, for every kind of regional protection available)*: ARIPO (BW, GH, GM, KE, LR, LS, MW, MZ, NA, RW, SD, SL, ST, SZ, TZ, UG, ZM, ZW), Eurasian (AM, AZ, BY, KG, KZ, RU, TJ, TM), European (AL, AT, BE, BG, CH, CY, CZ, DE, DK, EE, ES, FI, FR, GB, GR, HR, HU, IE, IS, IT, LT, LU, LV, MC, MK, MT, NL, NO, PL, PT, RO, RS, SE, SI, SK, SM, TR), OAPI (BF, BJ, CF, CG, CI, CM, GA, GN, GQ, GW, KM, ML, MR, NE, SN, TD, TG).

Published:

— *with international search report (Art. 21(3))*

(54) Title: HYPERSPECTRAL IMAGING FOR PREDICTION OF SKIN INJURY AFTER EXPOSURE TO THERMAL ENERGY OR IONIZING RADIATION

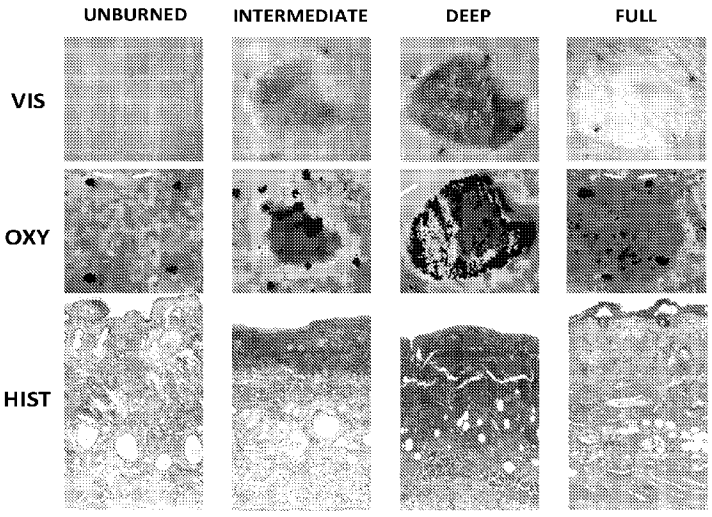

FIG. 6

(57) Abstract: The invention provides hyperspectral imaging-based methods that enable effective, efficient and non-invasive detection and characterization of thermal and ionizing radiation exposure in tissue. The methods allow for complete visualization and quantification of oxygenation and perfusion changes in thermal burn or ionizing radiation impacted skin and enables rapid identification of individuals exposed to such exposures and allows early prediction of extent of injury in normal tissue after exposure.

WO 2015/187489 A1

HYPERSPECTRAL IMAGING FOR PREDICTION OF SKIN INJURY AFTER EXPOSURE TO THERMAL ENERGY OR IONIZING RADIATION

Priority Claims and Related Patent Applications

[0001] This application claims the benefit of priority from U.S. Provisional Application Serial No. 62/007,891, filed on June 4, 2014, the entire content of which is incorporated herein by reference in its entirety.

Technical Fields of the Invention

[0001] The invention generally relates to methods for detecting and analyzing exposure of tissue to thermal burn or ionizing radiation. More particularly, the invention relates to methods for characterization, evaluation and prediction of injuries from thermal or radiation exposures in tissue and their effect thereof using hyperspectral imaging-based techniques.

Background of the Invention

[0002] Exposure to thermal burn or ionizing radiation can have profound biological consequences to skin and underlying subcutaneous tissue. Skin structures, especially the dermal plexus, demonstrate changes in response to both thermal and ionizing radiation energy. After exposure to thermal energy, depth of burn injury predicts the healing of the burn wound, and thus early and accurate assessment is of great importance in the care of the burn patient.

[0003] Thermal injury is divided into four degrees of depth or severity: superficial, superficial-partial, deep-partial, and full thickness burns. For full thickness and deep dermal burns, early excision and skin grafting of full thickness and deep dermal burns has been shown to be therapeutically and financially advantageous, with shorter healing time, fewer infections, better functional and aesthetic results, as well as reduced hospital stay and lower treatment cost. (Feller, *et al.* **1980** *JAMA* 244.18: 2074-2078; Herndon, *et al.* **1989** *Annals of Surgery* 209.5: 547; Ong, *et al.* **2006** *Burns* 32.2: 145-150; Heimbach, *et al.* **1992** *World Journal of Surgery* 16.1: 10-15; Prasanna, *et al.* **1994** *Burns* 20.5: 446-450; Burke, *et al.* **1976** *The Surgical clinics of North America* 56.2: 477-494.)

[0004] Early excision and skin grafting of full-thickness and deep dermal burns has been shown to be therapeutically and financially advantageous, with shorter healing time, fewer infections, better functional and aesthetic results, as well as reduced hospital stay. However, early differentiation of superficial dermal versus deep dermal burns presents a diagnostic challenge. Superficial and intermediate dermal burns heal with conservative management within two to three weeks. However, deep dermal burns result in prolonged hospitalizations, increased risk of infection, excessive scarring and thus are best managed by excision and skin grafting. (Johnson, *et al.* **2003** *Advances in Skin &*

Wound Care 16.4: 178-187; Jaskille, *et al.* **2009** *Journal of Burn Care & Research* 30.6: 937-947.) Differentiation between dermal burns that spontaneously heal versus those that require excision remains clinically challenging, with only 50-75% accuracy in early clinical assessments. (Heimbach, *et al.* **1992** *World Journal of Surgery* 16.1: 10-15; Alsbjörn, *et al.* **1984** *Scandinavian Journal of Plastic and Reconstructive Surgery and Hand Surgery* 18.1: 75-79; Niazi, *et al.* **1993** *Burns* 19.6: 485-489; Pape, *et al.* **2001** *Burns* 27.3: 233-239; Droog, *et al.* **2001** *Burns* 27.6: 561-568.)

[0005] Current standard of care involves waiting for progression of burn injury over the course of days until it becomes clinically evident whether spontaneous healing will occur or excision and grafting is required. Basic clinical overestimation of burn depth results in unnecessary surgery, while underestimation results in prolonged hospital stays, increased morbidity and mortality, delayed surgery, and inferior functional and aesthetic outcomes.

[0006] Thus, early reliable differentiation between superficial and deep dermal burns remains a top priority in burn research. In addition, current fluid resuscitation formulas are based on visual estimates of total body surface area burned. Over or under-estimation of burn injury results in inappropriate fluid resuscitation of the patient and potentially life threatening complications. (Heimbach, *et al.* **1992** *World Journal of Surgery* 16.1: 10-15; Johnson, *et al.* **2003** *Advances in Skin & Wound Care* 16.4: 178-187; Jaskille, *et al.* **2009** *Journal of Burn Care & Research* 30.6: 937-947; Alsbjörn, *et al.* **1984** *Scandinavian Journal of Plastic and Reconstructive Surgery and Hand Surgery* 18.1: 75-79; Niazi, *et al.* **1993** *Burns* 19.6: 485-489; Pape, *et al.* **2001** *Burns* 27.3: 233-239; Droog, *et al.* **2001** *Burns* 27.6: 561-568; Hoeksema, *et al.* **2009** *Burns* 35.1: 36-45; Park, *et al. Burns* (2013) 655-661.)

[0007] Among the various modalities to distinguish burns, histology remains the gold standard. Due to iatrogenic injury and sampling error potential, however, it has little application in actual clinical practice. (Heimbach, *et al.* **1992** *World Journal of Surgery* 16.1: 10-15; Jaskille, *et al.* **2009** *Journal of Burn Care & Research* 30.6: 937-947; Droog, *et al.* **2001** *Burns* 27.6: 561-568; Hoeksema, *et al.* **2009** *Burns* 35.1: 36-45.).

[0008] In addition, exposure to ionizing radiation can also have profound biological consequences to the skin. Scenarios for radiation exposure range from external beam radiotherapy for oncologic treatment to uncontrolled release events such as a nuclear attack or accident. The disasters it the Fukushima and Chernobyl emphasize the real possibility of the latter scenario. Cutaneous skin reactions in response to ionizing radiation exposure are major consequences in both cases. These skin reactions in the acute phase can range from mild skin erythema to ulceration. For radiotherapy alone, it has been reported that a majority of patients receiving radiotherapy experience some degree of skin reaction. (Murray *et al.* **2011** *Radiother Oncol.* 99(2):231-4)

[0009] With regard to radiation, two significant issues remain unaddressed: (1) the relationship between the dose of cutaneous irradiation and the magnitude of cutaneous perfusion changes observed over time, and (2) the relationship between early cutaneous perfusion changes and the development of acute or chronic skin injury post-irradiation. The latter posses a significant clinical problem since the development of acute skin reactions during radiotherapy usually signal a treatment break. It has been estimated that a treatment break of a more than a week during breast cancer radiotherapy can have significant negative impact on recurrence rate and overall survival. (Bese, *et al.* **2007** *Journal of BUON: official journal of the Balkan Union of Oncology*12(3):353-9. Bese, *et al.* **2005** *Oncology*. 69(3):214-23)

[0010] The ability to detect and predict high-risk areas for developing skin reactions and change the treatment plan may prevent the need for these detrimental treatment breaks.

[0011] Therefore, an urgent need continues to exist for effective, efficient, non-invasive methods for detection and characterization of both thermal burn and ionizing radiation exposure in tissue.

Summary of the Invention

[0012] The invention is based on the discovery of hyperspectral imaging-based methods that enable effective, efficient and non-invasive detection, characterization and prediction of the effect of thermal and ionizing radiation exposure in tissue. Methods of the invention allow for complete visualization and quantification of oxygenation and perfusion changes in thermal burn or ionizing radiation impacted skin. The invention enables rapid identification of individuals exposed to such exposures and allows early prediction of extent of injury in normal tissue after exposure.

[0013] In one aspect, the invention generally relates to a method for predicting a maximal depth of thermal burn injury formation in superficial tissue of a subject. The method includes: acquiring photographic imagery of one or more areas of superficial tissue of the subject at one or more wavelengths of light and one or more time points; and characterizing the obtained photographic imagery to measure one or more physiological properties in the one or more areas of superficial tissue to predict the maximal depth of burn injury formation in superficial tissue of the subject.

[0014] In another aspect, the invention generally relates to a biomedical imaging method for predicting acute skin reactions after exposure to ionizing radiation. The method includes: acquiring photographic imagery of one or more areas of superficial tissue of the subject at one or more wavelengths of light and one or more time points; and characterizing the obtained photographic imagery to detect changes in tissue oxygenation and perfusion levels of the subject to predict acute skin reactions.

[0015] In yet another aspect, the invention generally relates to a biomedical imaging method for predicting acute skin reactions after exposure to thermal injury. The method includes: acquiring photographic imagery of one or more areas of superficial tissue of the subject at one or more wavelengths of light and one or more time points; and characterizing the obtained photographic imagery to detect changes in tissue oxygenation and perfusion levels of the subject to predict acute skin reactions.

Brief Description of the Drawings

[0016] **FIG. 1**: Relative vessel density at 4 weeks after radiation dose demonstrated an inverse linear relationship with initial radiation dose exposure. ($r=0.90$, $p<0.0001$)

[0017] **FIG. 2**: Relative deoxyhemoglobin changes decreased over the the first 3 days for each level of radiation exposure. Note the increasing rate of change as the radiation dose becomes larger.

[0018] **FIG. 3**: Deoxyhemoglobin trend over the first three days for each dose level revealed a strong linear relationship. ($r=0.98$, $p<0.0001$)

[0019] **FIG. 4**: The final 4-week relative vessel density demonstrated a strong inverse relationship with initial three day deoxyhemoglobin slope for each radiation dose. ($r= 0.91$, $p<0.0001$)

[0020] **FIG. 5**: Maximal skin reaction score by day 14 was strongly correlated to the initial three day deoxyhemoglobin slope for each radiation dose. ($r=0.98$, $p<0.0001$)

[0021] **FIG. 6:** Macroscopic, histological, and vsHSI comparisons at three days post burn. Left to right columns are unburned skin, intermediate dermal burn, deep dermal burn, and full-thickness burn. Rows top to bottom are gross view, vsHSI (OxyHb parameter), histology 10X magnification and stained with Masson's trichrome.

[0022] **FIG. 7:** Total Hemoglobin (tHb) Variations in Three Depths of Burn. tHb is relative to its pre-burn baseline for the three depths of burn, measured over the first 72 hours post injury. All values are expressed as mean ± standard deviation of the mean. Statistical significance of $p<0.05$ between ID and DD burns is indicated with an (*) asterisk.

[0023] **FIG. 8:** Deoxygenated Hemoglobin (DeOxyHb) Variations in Three Depths of Burn. DeOxyHb is relative to its pre-burn baseline for the three depths of burn, measured over the first 72 hours post injury. All values are expressed as mean ± standard deviation of the mean. Statistical significance of $p<0.05$ between ID and DD burns is indicated with an (*) asterisk.

[0024] **FIG. 9:** Oxygenated Hemoglobin (OxyHb) Variations in Three Depths of Burn. OxyHb is relative to its pre-burn baseline for the three depths of burn, measured over the first 72 hours

post injury. All values are expressed as mean ± standard deviation of the mean. Statistical significance of $p<0.05$ between ID and DD burns is indicated with an (*) asterisk.

[0025] **FIG. 10:** Oxygen Saturation (SatO2) Variations in Three Depths of Burn. SatO2 is relative to its pre-burn baseline for the three depths of burn, measured over the first 72 hours post injury. All values are expressed as mean ± standard deviation of the mean. Statistical significance of $p<0.05$ between ID and DD burns is indicated with an (*) asterisk.

[0026] **FIG. 11**: Oxygen Saturation (SatO2) compared to final burn depth. SatO2 at 1 hour plotted against final burn depth 72 hours post injury demonstrates a non-linear correlation ($R^2=0.99975$, $p<0.001$).

Detailed Description of the Invention

[0027] The invention provides hyperspectral imaging-based methods that enable effective, efficient and non-invasive detection, characterization and prediction of the effect of thermal and ionizing radiation exposure in tissue. By complete visualization and quantification of oxygenation and perfusion changes in thermal burn or ionizing radiation impacted skin, the method of the invention enables rapid identification of individuals exposed to such exposures and allows early prediction of extent of injury in normal tissue after exposure.

[0028] Thermal injury is divided into four degrees of depth or severity: superficial, superficial-partial, deep-partial, and full thickness burns. First-degree burns, also called superficial burns, only involve the uppermost layer of skin, the epidermis. These burns heal within days and do not result in scarring. A blistering sunburn is an example of a superficial burn. Second-degree burns involve the entire epidermis and part of the dermis. Depending on the extent of dermal involvement, these burns may be further divided into superficial and deep partial thickness burns. While superficial-partial burns generally heal without surgical intervention, deep-partial thickness burns may resist healing and surgical intervention may be required. Third degree, or full-thickness, burns require surgical excision and subsequent skin grafting.

[0029] A promising parameter for burn depth assessment is its correlation with skin perfusion: superficial burn injury causes an inflammatory response and thus increased perfusion to the burn site, while deeper burns are prone to destroy the dermal microvasculature and thus a decrease in perfusion follows. Furthermore, the distinction between destroyed versus preserved blood supply has impact over the future viability and recovery of tissue. However, despite advances in the field of burn diagnostics, a reliable non-invasive method to aid in early burn depth diagnosis still does not exist. (Alsbjörn, *et al.* **1984** *Scandinavian Journal of Plastic and Reconstructive Surgery and Hand Surgery* 18.1: 75-79; Niazi, *et al.* **1993** *Burns* 19.6: 485-489; Pape, *et al.* **2001** *Burns* 27.3: 233-239; Droog, *et al.* **2001** *Burns* 27.6: 561-568; Park, *et al. Burns* (2013) 655-661; Monstrey,

et al. **2008** *Burns* 34.6: 761-769; Qin, *et al.* **2012** *Biomedical Optics Express* 3.3: 455-466; Sowa, *et al.* **2001** *Burns* 27.3: 241-249; Cross, *et al.* **2007** *Wound Repair and Regeneration* 15.3: 332-340.)

[0030] Exposure to ionizing radiation can also have profound biological consequences to the skin. Scenarios for radiation exposure range from external beam radiotherapy for oncologic treatment to uncontrolled release events such as a nuclear attack or accident. The disasters it the Fukushima and Chernobyl emphasize the real possibility of the latter scenario. Cutaneous skin reactions in response to ionizing radiation exposure are major consequences in both cases. These skin reactions in the acute phase can range from mild skin erythema to ulceration. For radiotherapy alone, it has been reported that a majority of patients receiving radiotherapy experience some degree of skin reaction. (Murray, *et al.* **2011** *Radiother Oncol.* 99.2: 231-4.)

[0031] The precise etiology of ionizing radiation-induced skin injury remains unclear. Multiple theories proposed include direct cellular injury, cell signaling dysregulation, and ischemia. Recently, the literature has suggested that cutaneous ischemia may be the predominant characteristic that links both acute and chronic-phase injuries. However, these studies have all been limited as they use only a single large dose of ionizing radiation. (Marx, *et al.* **1990** *Am J Surg.* 160.5:519-24; Martin, *et al.* **2000** *Int J Radiat Oncol Biol Phys.* 47.2: 277-90; Aitasalo, *et al.* **1986** *Plast Reconstr Surg.* 77.2: 256-67; Thanik, *et al.* **2011** *Plast Reconstr Surg.* 127.2: 560-8; Doll, *et al.* **1999** *Radiother Oncol.* 51.1: 67-70.)

[0032] Recently, a novel method for assessing radiation-induced skin injury has been reported. (Chin, *et al.* **2012** *Journal of Biomedical Optics.* 17.2: 026010; Chin, *et al.* **2013** *Plast Reconstr Surg.* 131.4: 707-16; WO 2013/082192A1 by Chin) For example, using a hairless mouse and a single fixed-dose of surface beta-irradiation, a reliable model of radiation-induced skin injury has been generated. Using hyperspectral imaging technology, characteristic changes have been identified in cutaneous perfusion that are reproducible in magnitude and in timing, preceding the visible appearance of skin injury.

[0033] Two significant issues remain: (1) the relationship between the dose of cutaneous irradiation and the magnitude of cutaneous perfusion changes observed over time and (2) the relationship between the magnitude of early cutaneous perfusion changes observed over time and the development of acute skin injury post-irradiation. The latter posses a significant clinical problem since the development of acute skin reactions during radiotherapy usually signals a treatment break. It has been estimated that a treatment break of more than a week during breast cancer radiotherapy can have significant negative impact on recurrence rate and overall survival. (Bese, *et al.* **2007** *Journal of BUON* 12.3: 353-9; Bese, *et al.* **2005** *Oncology.* 69.3: 214-23.)

Therefore, the ability to detect and predict high-risk areas for developing skin reactions and change the treatment plan may prevent the need for these detrimental treatment breaks.

[0034] Current standard of practice for evaluating burn injury involve visual estimation by clinical exam. Previous groups have demonstrated the ability of hyperspectral imaging to assess the current perfusion and oxygenation patterns of burned skin, but no predictive model for maximal burn depth was generated from this work. Hyperspectral imaging and other non-invasive techniques such as laser Doppler flowmetry have been used to demonstrate early changes in perfusion and oxygenation but no methods have been developed to use this information to predict a precise level of maximal burn depth which forms several days later. In addition, there are no existing methods for prediction of skin reactions (acute or chronic) after exposure to ionizing radiation.

[0035] A unique aspect of this invention is the application of an existing technology, hyperspectral imaging, to early prediction of injury in normal tissue after exposure to thermal injury or ionizing radiation. These normal tissues include skin and any external surface of the body, *e.g.*, eyes, nails, hair, *etc.* For thermal injury, maximum level of burn injury is defined as the percentage of dermis presenting with burn injury 72 hours after thermal exposure. The invention described herein utilizes hyperspectral imaging for the prediction of maximum level of burn injury in normal tissue as well as the prediction of acute and chronic skin reactions secondary to radiation exposure.

[0036] In particular, the invention employs changes in the spectral signature of skin, including those representative of oxy-hemoglobin and deoxy-hemoglobin levels, to assess thermal exposure and predict the depth of burn injury. The spectral signature is represented by selected specific wavelengths, for example, of visible and infrared light (*e.g.*, 350 nm -1200 nm). This invention allows us to utilize these detected changes to determine what tissue has been exposed to thermal burn and predict the clinical presentation of maximal depth of burn or ionizing radiation injury. Using the method disclosed herein, one can reliably predict the maximal depth of injury as early as 1 hour after thermal exposure, a task not possible with existing methods.

[0037] For radiation injury, acute skin injury is defined as an erythema, moist or dry desquamation, or ulceration that occurs days to weeks after radiation exposure. Chronic injury refers to fibrosis, decreased vasculature, and chronic ulceration that forms months to years later. The invention utilizes changes in the spectral signature of skin, including those representative of oxy-hemoglobin and deoxy-hemoglobin levels, to assess radiation exposure and predict acute and chronic skin reactions. The spectral signature is represented by selected specific wavelengths, for example, of visible and infrared light (*e.g.*, 350 nm -1200 nm). This invention allows us to utilize these detected changes to determine what tissue has been exposed to predict the clinical

presentation of acute or chronic skin injury. Using the method disclosed herein, one can reliably predict the maximal depth of injury as early as 72 hours hour after radiation, a task not possible with existing methods.

[0038] The novel method of the invention relies on changes in the oxy- and deoxy-hemoglobin levels as assessed by their reflectance and absorbance of visible light in areas of thermal and radiation exposure to predict subsequent injury. The disclosed method is rapid and non-invasive and the results are available at the point-of-care and allow for immediate triage and decision-making ability. With regards to the ability of hyperspectral imaging to characterize changes in perfusion and oxygenation in normal tissue, the invention allows for the simultaneous assessment of oxygenation and perfusion changes.

[0039] For burn patients and healthcare providers, the invention offers significant benefits including the early and accurate prediction of maximal level burn injury, for instance, in emergency department and trauma settings. Early assessment of maximal burn depths enables more accurate assessment of total body surface area burned and therefore guides fluid resuscitation. In addition, early prediction of thermal burns allows for close monitoring and earlier excision of full thickness burns thereby minimizing chances for complications such as major infection or septic shock. Early prediction of high-risk burn areas may also identify areas that might respond to mitigating therapeutics.

[0040] Major benefits of the disclosed method for skin reactions secondary to ionizing radiation include providing radiation oncologists with an indication for areas that are high risk for developing a skin reaction during the treatment course, which enable the oncologist to refine the treatment plan to avoid a skin reaction without a detrimental treatment break. Additionally, the method produces prediction of areas that may be prone to chronic ulceration or infection years later after exposure to ionizing radiation. This is particularly important to plastic surgeons who may be consulted to provide wound care treatment or reconstructive procedures to the affected area.

[0041] In one aspect, the invention generally relates to a method for predicting a maximal depth of thermal burn injury formation in superficial tissue of a subject. The method includes: acquiring photographic imagery of one or more areas of superficial tissue of the subject at one or more wavelengths of light and one or more time points; and characterizing the obtained photographic imagery to measure one or more physiological properties in the one or more areas of superficial tissue to predict the maximal depth of burn injury formation in superficial tissue of the subject.

[0042] In certain embodiments, the one or more physiological properties are selected from tissue oxygenation and perfusion levels after exposure to thermal injury.

[0043] The one or more wavelengths of light may be any suitable wavelength, for example, selected from the range from about 350 nm to about 1,200 nm (*e.g.*, from about 350 nm to about 900 nm, from about 350 nm to about 700 nm, from about 400 nm to about 1,200 nm, from about 550 nm to about 1,200 nm).

[0044] The photographic imagery may be obtained at a time suitable for the application at hand. In certain embodiments, the photographic imagery is obtained within a time frame from about 1 hour to about 48 hours (*e.g.*, from about 1 hour to about 36 hours, from about 1 hour to about 24 hours, from about 1 hour to about 24 hours, from about 1 hour to about 12 hours, from about 1 hour to about 6 hours, from about 1 hour to about 3 hours, from about 6 hours to about 48 hours, from about 6 hours to about 36 hours, from about 6 hours to about 24 hours, from about 6 hours to about 12 hours) after a thermal exposure to predict the maximum burn depth. In certain embodiments, the photographic imagery is obtained within a time frame from about 6 hours to 1 day after a thermal exposure. In certain embodiments, the photographic imagery is obtained after 1 day after a thermal exposure.

[0045] In certain embodiments, measuring one or more physiological properties includes detecting and quantifying the level of oxygenated hemoglobin and an increase or decrease in measured levels of oxygenated hemoglobin in the burned area of the subject is used as a biomarker to predict maximum burn depth.

[0046] In certain embodiments, measuring one or more physiological properties includes detecting and quantifying the level of de-oxygenated hemoglobin and an increase or decrease in measured levels of de-oxygenated hemoglobin in burned area of a subject is used as a biomarker to predict maximum burn depth.

[0047] In certain embodiments, measuring one or more physiological properties comprises detecting and quantifying the level of tissue oxygen saturation and an increase or decrease in measured levels of tissue oxygen saturation in the burned area of a subject is used as a biomarker to indicate predict maximum burn depth.

[0048] In certain embodiments, measuring one or more physiological properties comprises detecting and quantifying the level of total hemoglobin and an increase or decrease in measured levels of total hemoglobin in the burned area of a subject is used as a biomarker to predict maximum burn depth.

[0049] Characterization of the obtained photographic imagery may be performed in conjunction with assessment of collagen, lipids, water, or another naturally occurring molecules.

[0050] In certain embodiments, the method further includes characterizing the obtained photographic imagery to measure one or more physiological properties in the one or more areas of superficial tissue to estimate total body surface area of a patient's burned skin.

[0051] In another aspect, the invention generally relates to a biomedical imaging method for predicting acute skin reactions after exposure to ionizing radiation. The method includes: acquiring photographic imagery of one or more areas of superficial tissue of the subject at one or more wavelengths of light and one or more time points; and characterizing the obtained photographic imagery to detect changes in tissue oxygenation and perfusion levels of the subject to predict acute skin reactions.

[0052] Various acute skin reactions can be detected and evaluated by the method of the invention, for example, erythema, moist or dry desquamation, or ulceration.

[0053] The one or more wavelengths of light may be any suitable wavelength, for example, selected from the range from about 350 nm to about 1,200 nm (*e.g.*, from about 350 nm to about 900 nm, from about 350 nm to about 700 nm, from about 400 nm to about 1,200 nm, from about 550 nm to about 1,200 nm).

[0054] The photographic imagery may be obtained at a time suitable for the application at hand. In certain embodiments, the photographic imagery is obtained within a time frame from about 3 to about 5 days (*e.g.*, about 3 days, about 4 days, about 5 days) after exposure to ionizing radiation to predict acute skin reaction occurring within one month.

[0055] In certain embodiments, measuring one or more physiological properties comprises detecting and quantifying oxygenated hemoglobin levels and an increase or decrease in measured levels of oxygenated hemoglobin in the exposed area of a subject is used as a biomarker to predict acute skin reaction.

[0056] In certain embodiments, measuring one or more physiological properties comprises detecting and quantifying de-oxygenated hemoglobin levels and an increase or decrease in measured levels of de-oxygenated hemoglobin in the exposed area of a subject is used as a biomarker to predict acute skin reaction.

[0057] In certain embodiments, measuring one or more physiological properties comprises detecting and quantifying the level of tissue oxygen saturation and an increase or decrease in measured levels of tissue oxygen saturation in the burned area of a subject is used as a biomarker to indicate predict acute skin reaction.

[0058] In certain embodiments, measuring one or more physiological properties comprises detecting and quantifying the level of total hemoglobin and an increase or decrease in measured levels of total hemoglobin in the burned area of a subject is used as a biomarker to predict acute skin reaction.

[0059] Characterization of the obtained photographic imagery may be performed in conjunction with assessment of collagen, lipids, water, or another naturally occurring molecules.

[0060] In yet another aspect, the invention generally relates to a biomedical imaging method for predicting acute skin reactions after exposure to thermal injury. The method includes: acquiring photographic imagery of one or more areas of superficial tissue of the subject at one or more wavelengths of light and one or more time points; and characterizing the obtained photographic imagery to detect changes in tissue oxygenation and perfusion levels of the subject to predict acute skin reactions.

[0061] Various acute skin reactions can be detected and evaluated by the method of the invention, for example, erythema, moist or dry desquamation, or ulceration.

[0062] The one or more wavelengths of light may be any suitable wavelength, for example, selected from the range from about 350 nm to about 1,200 nm (*e.g.*, from about 350 nm to about 900 nm, from about 350 nm to about 700 nm, from about 400 nm to about 1,200 nm, from about 550 nm to about 1,200 nm).

[0063] The photographic imagery may be obtained at a time suitable for the application at hand. In certain embodiments, the photographic imagery is obtained within a time frame from about 1 hour to about 48 hours (*e.g.*, from about 1 hour to about 36 hours, from about 1 hour to about 24 hours, from about 1 hour to about 24 hours, from about 1 hour to about 12 hours, from about 1 hour to about 6 hours, from about 1 hour to about 3 hours, from about 6 hours to about 48 hours, from about 6 hours to about 36 hours, from about 6 hours to about 24 hours, from about 6 hours to about 12 hours) after a thermal exposure to predict the maximum burn depth. In certain embodiments, the photographic imagery is obtained within a time frame from about 6 hours to 1 day after a thermal exposure. In certain embodiments, the photographic imagery is obtained after 1 day after a thermal exposure.

[0064] In certain embodiments, measuring one or more physiological properties includes detecting and quantifying the level of oxygenated hemoglobin and an increase or decrease in measured levels of oxygenated hemoglobin in the burned area of the subject is used as a biomarker to predict maximum burn depth.

[0065] In certain embodiments, measuring one or more physiological properties includes detecting and quantifying the level of de-oxygenated hemoglobin and an increase or decrease in measured levels of de-oxygenated hemoglobin in burned area of a subject is used as a biomarker to predict maximum burn depth.

[0066] In certain embodiments, measuring one or more physiological properties comprises detecting and quantifying the level of tissue oxygen saturation and an increase or decrease in measured levels of tissue oxygen saturation in the burned area of a subject is used as a biomarker to indicate predict maximum burn depth.

[0067] In certain embodiments, measuring one or more physiological properties comprises detecting and quantifying the level of total hemoglobin and an increase or decrease in measured levels of total hemoglobin in the burned area of a subject is used as a biomarker to predict maximum burn depth.

[0068] Characterization of the obtained photographic imagery may be performed in conjunction with assessment of collagen, lipids, water, or another naturally occurring molecules.

[0069] The subject may be any suitable species, including a human and a non-human animal.

[0070] A computer and algorithm may be included in the system for image processing and data analysis, particularly in characterizing the obtained photographic imagery.

[0071] In certain embodiments, the method further includes determining course of medical treatment or segregation of individual subjects into groups for triage in a mass casualty scenario. In certain embodiments, the method further includes segregating individual subjects into groups for triage in a mass casualty scenario.

[0072]

Examples

Example 1. Hyperspectral Imaging as an Early Biomarker for Radiation Exposure and Microcirculatory Damage

[0073] The study demonstrates that early measurement of cutaneous deoxygenated hemoglobin levels after radiation exposure is a useful biomarker for dose reconstruction and also for chronic microvascular injury. Changes in deoxygenated hemoglobin can also be correlated to acute skin reactions before any are visible.

Animals and Irradiation Procedure

[0074] All handling of and procedures performed with animals was done in accordance with a protocol (UMass IACUC Protocol #A2354) approved by our Institutional Animal Care and Use Committee. Prior to this experiment, a model of acute radiation-induced skin injury was established. (Chin, *et al.* **2012** *J. Biomedical Optics* 17(2):026010.) The radiation source utilized was a Strontium-90 beta-emitter with an active diameter of 9 mm, which created an 8 mm diameter skin injury. This beta-emitter source delivers less than 10% of the total dose deeper than 3.6 mm into the skin, avoiding injury to internal organs.

[0075] Hairless, immunocompetent adult mice (SKH-1 Elite, Charles River Laboratories, Wilmington, MA) were used. Mice (n=66) were equally divided into 6 groups. Mice received one of six pre-specified doses of ionizing radiation respectively: 0, 5, 10 , 20, 35, and 50 Gy.

[0076] On day 0 mice were anesthetized. Tattooing was performed bilaterally on the dorsal flank skin of the mice to act as fiducial marks. Cutaneous perfusion was assessed using HSI prior to irradiation as described below. This pre-irradiation assessment served as a baseline level for subsequent comparison. Mice then received a single pre-specified dose of irradiation as described above. Accurate dose-delivery was ensured prior to animal irradiation using radiochromic film dosimetry. Following irradiation, mice were recovered and housed individually.

Hyperspectral Imaging for Evaluation of Cutaneous Perfusion

[0077] Evaluation of cutaneous perfusion was accomplished using a novel application of an existing technology, HSI. HSI is a method of wide-field diffuse reflectance spectroscopy that utilizes a spectral separator to vary the wavelength of light entering a digital camera and provides a diffuse reflectance spectrum for every pixel. These spectra are then compared to standard transmission solutions to calculate the concentration of deoxy-hemoglobin (DeoxyHb) in each pixel, from which spatial maps of these parameters are constructed.

[0078] Using HSI, cutaneous perfusion was analyzed over the first three days after radiation exposure. Skin reactions were then evaluated twice weekly for the first 14 days and then weekly through 28 days post-irradiation. At the time of each evaluation, mice were anesthetized and maintained at standard body temperature. The OxyVu-2 device (HyperMed, Greenwich, CT) was utilized for HSI acquisitions. The OxyVu-2-generated spatial maps of tissue DeoxyHb were used for quantification of cutaneous perfusion. These maps were analyzed with MATLAB R2010b (Mathworks Inc., Natick, MA). Mean values of DeoxyHb were calculated for a 79-pixel area corresponding to the irradiated area on each flank. This 79-pixel area was determined precisely over time with reference to the fiducial tattoo marks that were placed prior to irradiation.

[0079] Similarly, areas of non-irradiated contralateral flank skin were quantified to ensure that any changes in perfusion observed in the irradiated skin were not due to natural variations or systemic phenomena.

[0080] Values for DeoxyHb parameters for post-irradiation time points are expressed as relative to pre-irradiation values within the same area of skin. Mean relative values reported hereafter reflect the average of relative levels for all subjects within a dose group at a specified timepoint.

Post-Irradiation Tissue Analysis

[0081] On day 28 post-irradiation, mice were euthanized following cutaneous perfusion assessment. Immediately post-mortem, irradiated and non-irradiated skin from both flanks was harvested. Tissue was fixed en bloc in 10% neutral-buffered formalin solution and kept at 4 °C

overnight for paraffin embedment. Paraffin-embedded sections were re-hydrated though a decreasing alcohol series and stained for vasculature as described previously. (Chin, *et al.* **2013** *Plast Reconstr Surg*. 131(4):707-16.) Primary antibody (PECAM-1) for vasculature staining (BD Pharmingen, San Jose, CA) was incubated at 4°C overnight. Signals were intensified by using a tyramide amplification system (PerkinElmer, Boston, MA) and activated with DAB Chromogen (Dako North America Inc., Carpinteria, CA). Slides were counterstained with hematoxylin.

[0082] Digital images were obtained from the center of all stained skin sections at 10x magnification with an Olympus BX53 microscope (Olympus America Inc., Center Valley, PA). Two blinded reviewers quantified vessel density using 3 random standard-sized fields and results were averaged. Vessel densities for each animal were expressed as a ratio between the irradiated sample and its respective contralateral non-irradiated internal control, yielding normalized mean vessel densities.

Statistical Analysis

[0083] For hyperspectral data, plots of perfusion data are expressed as the relative mean unless otherwise specified. Changes in DeoxyHb and dose were correlated with cutaneous blood vessel densities using linear regression models. Statistical significance was assumed for p values less than 0.05.

Macroscopic Skin Reaction

[0084] Mice were irradiated as previously described without complication. Mice gained weight appropriately following irradiation and no morbidity or mortality was observed. Skin reactions began forming in all groups by approximately one week post-irradiation. Maximal skin reactions were observed by day 14 in all groups and scored using the Radiation Therapy Oncology Group toxicity scoring system, which describes skin reactions from erythema to ulceration over a four-point scale. (Salvo, *et al.* **2010** *Current oncology* 17(4):94-112.) Maximal skin reactions were observed to be characterized by erythema in the 5 and 10 Gy groups. Dry desquamation was observed as the maximal skin reaction of mice receiving 20 and 35 Gy. In the 50 Gy group, moist desquamation was observed in all irradiated areas.

Changes in Microvascular Density

[0085] A pronounced reduction in cutaneous vascular densities at four weeks following irradiation was observed. CD31 immunohistochemistry demonstrated an inverse correlation ($r=0.90$, $p<0.0001$) between dose and vessel reduction severity, with vessel counts decreasing as the dose increased. (**FIG. 1**)

Relationship of Early Deoxygenated Hemoglobin Changes and Radiation Dose

[0086] Using HSI analysis, early changes in deoxygenated hemoglobin levels were observed during the first three days post-irradiation in all groups. An acute decrease in deoxygenated hemoglobin was seen for each dose over the first 3 days before any visible skin reactions were observed. (**FIG. 2**) When further examining the behavior of deoxygenated hemoglobin over the first 3 days, it was noted that the slope changed linearly with increasing radiation dose exposure ($r=0.98$, $p<0.0001$). (**FIG. 3**)

Correlation between Early Deoxygenated Hemoglobin Changes and Microvascular Density

[0087] Using the relationships between early DeoxyHb change with dose, it was also observed that deoxygenated hemoglobin decrease at 3 days had a strong linear association with microvascular density by 4 weeks for the given doses, indicating that early deoxygenated hemoglobin response could be predictive of final degree of microvascular damage. There was a highly significant correlation ($r= 0.91$, $p<0.0001$) between these early changes in deoxygenated hemoglobin and late vascular injury severity assessed. (**FIG. 4**)

Relationship between Early Deoxygenated Hemoglobin Changes and Skin Reaction

[0088] In addition, when examining the relationship between deoxygenated slope change in the first 3 days and maximal skin reaction at 14 days, there was a strong linear correlation ($r=0.98$, $p<0.0001$). (**FIG. 5**) This suggests that early decreases seen during serial assessment of deoxygenated hemoglobin may be related to the degree of maximal skin reaction after radiation exposure.

[0089] The current study demonstrated that over a large exposure gradient, the initial radiation dose appears to be directly correlated to the degree of microvascular injury. This finding is consistent with results by Haubener et al who showed that varying doses of single fraction radiation exposure had an increasing effect on diminishing endothelial cell number in vitro.

[0090] Furthermore, it was found that a strong relationship exists between deoxygenated hemoglobin response and final vessel density after radiation exposure. This suggests the possibility of using early monitoring of deoxygenated hemoglobin for prediction of chronic vascular damage.

[0091] In parallel, these results also indicate that deoxygenated hemoglobin response may be related to formation of acute skin reaction seen weeks after initial radiation exposure. No previous studies have been able to identify a biomarker that predicts the formation of an adverse skin reaction after exposure to radiation. If supported by clinical studies, applications of this finding could result in improved skin monitoring of patients receiving both therapeutic and

diagnostic radiologic procedures. Currently, the development of acute skin reactions during radiotherapy usually signals a treatment break. It has been estimated that a treatment break of a more than a week during breast cancer radiotherapy can negatively impact recurrence rate and overall survival. Therefore, the ability to detect and predict high-risk areas or high-risk patients for developing skin reactions earlier and change the treatment plan accordingly, may prevent the need for these detrimental treatment breaks.

Example 2. Hyperspectral Imaging as an Early Prediction of Maximal Burn Depth after Thermal Injury

[0092] This example was to characterize dermal perfusion and oxygenation in three sequential depths of burn over a dynamic, three-day period after burn injury, and to assess whether vsHSI could differentiate depths of injury, based on any of the parameters it quantifies: oxyHb, deoxyHb, tHb, or StO_2.

Animals and Thermal Burn Procedure

[0093] All handling of and procedures performed with animals was done in accordance with a protocol (UMass IACUC Protocol #A2454) approved by our Institutional Animal Care and Use Committee.

[0094] One hundred and seven hairless immune-competent, adult male mice (SKH-1 Elite, Charles River Laboratories, Wilmington, MA) were used. Anesthesia for thermal burn procedure and imaging was performed with a mixture of ketamine (55 mg/kg) and xylazine (5 mg/kg). Tattoo marks were placed on the dorsum of the mice to act as fiducial marks. After anesthesia, the dorsal skin was distracted from the body, and a 1.5 cm diameter brass rod of 82 grams heated to 50 (n=12), 55 (n=12), 60 (n=26), 70 (n=23), 80 (n=12), or 90°C (n=22) was applied to the dorsum of the anesthetized mice (gravity only) for 10 seconds creating thermal injury of graded severity. Animals received subcutaneous, slow release buprenorphine (0.2 mg/kg) and intraperitoneal 1 ml of normal saline after the burn procedure. Twelve mice randomly selected from each burn group were sacrificed at 72 hours after burn injury (n=72) and biopsy samples were taken for histological analysis. The rest were sacrificed at a later timepoint out of the scope of this paper.

Histological burn depth analysis

[0095] Punch skin biopsies were taken from the center of burns at 72 hours post injury to evaluate burn progression over the first 3 days post injury. (Jackson **1953** *The British Journal of Surgery* 40(164):588-596; Tobalem, *et al.* **2013** Journal of Plastic, Reconstructive & Aesthetic Surgery 66(2):260-266.) Biopsies fixed in buffered formalin, embedded in paraffin and 10 micron

sections stained with Masson's Trichrome, a stain favorable in partial burns due to its magenta-red coloring of denatured collagen, indicative of the extent of the burn. (Chvapil, *et al.* **1984** *Plastic and Reconstructive Surgery* 73(3):438-441.) Images were taken with an Olympus microscope at 10X magnification. Burn depth was measured with a linear tool of Image J from every picture at three places in each image: left, center, and right. Percent burn depth was defined as depth of denatured collagen divided by depth to Panniculus Carnosus muscle x 100. Averages were taken of all the depths measured for each temperature of burn.

Evaluation of Cutaneous Perfusion and Oxygenation with Hyperspectral Imaging in the Visible Spectrum (vsHSI)

[0096] Perfusion and oxygenation parameters of the injured skin were measured with vsHSI, a non-invasive method of wide-field, diffuse reflectance spectroscopy at baseline before the burn, and at 2 minutes, 1 hour, 24 hours, 48 hours, and 72 hours after burn injury.

[0097] The OxyVu2™ device (HyperMed, Greenwich, CT) utilizes a spectral separator to vary the wavelength of visible light entering a digital camera and provides a diffuse reflectance spectrum for every pixel. These spectra are then compared to standard transmission solutions to calculate the concentration of oxygenated hemoglobin (oxyHb) and deoxygenated hemoglobin (deoxyHb) in each pixel, from which spatial maps of these parameters are constructed and used for quantification of cutaneous perfusion and oxygenation. These maps were analyzed with MATLAB R2010b (Mathworks Inc., Natick, MA). Mean values of oxyHb and deoxyHb were calculated for a 79-pixel area corresponding to the burned skin. This 79-pixel area was determined precisely over time with reference to the fiducial tattoo marks that were placed prior to burn injury. OxyHb and deoxyHb values were summed to yield total tissue hemoglobin (tHb), which represents total blood volume and thus total perfusion in the area of skin examined. Tissue oxygen saturation (StO_2) was calculated as oxyHb divided by tHb.

[0098] Post-burn oxyHb, deoxyHb, tHb, and StO_2 values are expressed as relative to pre-burn values within the same area of skin to account for oxygenation differences between animals at baseline.

Statistical analysis

[0099] Descriptive statistics were conducted on all of the measures of hemoglobin concentration: oxyHb, deoxyHb, tHb and StO_2 at the burn site at each time point, including 2 minutes, 1 hour, 24 hours, 48 hours and 72 hours following the induced burn. A series of Kruskal Wallis tests were used to determine whether there are any significant differences in hemoglobin concentration measures by the class of burn. A separate test for each measure of hemoglobin concentration at each separate time measure was performed. Non-parametric post-hoc Wilcoxon

rank sum tests comparing whether a hemoglobin measure was different between two specific classes of burn at the same time point was applied. Post-hoc tests were only conducted when the omnibus Kruskallis Wallis test found a significant difference in hemoglobin measures by the 3 classes of burn: intermediate dermal, deep dermal, and full-thickness. All statistical tests were performed using Stata 13 (StataCorp. 2013. *Stata Statistical Software: Release 13*. College Station, TX: StataCorp LP).

Histological Assessment

[00100] Three discrete levels of burn depth were identified histologically. Fifty-degree and fifty-five degree Celsius groups produced no injury. The sixty-degree group resulted in 58% (±18%) of dermal damage that was classified as intermediate dermal (ID) burn. Seventy-degree group resulted in 80% (± 14%) of dermal damage, which was classified as deep dermal (DD) burn. Both eighty and ninety-degree groups resulted in full-thickness (FT) injury 95% (± 13%) and 99% (± 2%), respectively (**FIG. 6**).

Evaluation of Cutaneous Perfusion and Oxygenation with vsHSI

[00101] **Total Hemoglobin (tHb).** The ID burn group exhibited a rise in tHb beginning at 2 minutes post injury, peaked at 48hrs with a 1.73 fold increase over baseline, and continued to be elevated until the end of the experiment at 72 hours with a 1.53 fold increase over baseline. The DD group also exhibited an increase in tHb over baseline levels, though to a lesser extent than the ID group, with a tHb peak at 48 hours of 1.25 fold increase over baseline levels and a 1.22 increase at 72 hours. FT injury had a fall in tHb beginning at 1 hour with tHb being 0.67 of baseline levels and reached the lowest point at 24 hours with 0.36 of baseline levels; at 72 hours tHb levels were 0.44 of original levels (**FIG. 7**). tHb was statistically different ($p<0.05$) between ID and DD as well as DD and FT at all time points; it was also significant between ID and FT at all timepoints except at the 2 minute mark.

[00102] **Oxygenated and Deoxygenated Hemoglobin. FIG. 9** shows the changes in deoxygenated hemoglobin (deoxyHb) and **FIG. 10**, changes in oxygenated hemoglobin (oxyHb), of each burn depth, over 72 hours post injury. The ID burn group had the greatest rise in both oxyHb and deoxyHb. ID group's oxyHb peaked at 48 hours at 1.34 fold increase over baseline, and its deoxyHb peaked at 24 hours with 1.52 increase. DD burn group had a peak of oxyHb at 1 hour at 1.69 over baseline, and then it trended down, with 1.32 over original levels at 72 hours. DD's deoxyHb initially decreased after injury, with 0.63 of baseline levels, at 1 hour. Then it increased to pre-burn levels by 24 hours, and to 1.20 above baseline levels at 48 and 72 hours. FT burn group had an increase in oxyHb of 1.48 at 1 hour, followed by a decrease with 0.48-0.50 of baseline levels at 24, 48, and 72 hours. The deoxyHb in the FT group decreased at 1 hour to

0.36 and at 24 hours to 0.31 of baseline levels; at 48 and 72 hours deoxyHb recovered slightly to 0.38 and 0.44 of baseline levels, respectively (**FIG. 8** and **FIG. 9**). DeoxyHb was statistically different ($p<0.05$) between ID and DD at all but the 2 minute and 72 hour time points, and between DD and FT as well as ID and FT, at all but the 2 minute time point. OxyHb was significant between the ID and DD groups at 48 and 72 hours, and between the DD and FT as well as ID and FT, at 24, 48, and 72 hours.

[00103] **Oxygen Saturation. FIG. 11** depicts saturation changes in the three burn-depth groups post injury. At 1-hour post injury, FT group had the greatest increase in saturation, 2.08 (± 0.64) fold increase over baseline. DD exhibited a 1.74 (± 0.36) fold increase and ID, a 1.44 (± 0.62) fold increase over baseline (**FIG. 10**). At 1-hour, there is a statistically significant difference between burn groups ID and DD, $p<0.05$, groups DD and FT, $p<0.05$, and groups ID and FT, $p<0.001$. The only other statistically significant time point for oxygen saturation characteristics was at 72 hours, between ID and DD ($p<0.05$) and DD and FT ($p<0.01$).

Assessing Early Differences between Burn Groups

[00104] **Intermediate Dermal (ID) versus Deep Dermal (DD).** Intermediate versus deep dermal perfusion measurements were statistically different at 1 hour for the following parameters: deoxyHb, ($p < 0.001$); tHb, ($p < 0.01$); and oxygen saturation (StO_2), ($p<0.05$). oxyHb did not differentiate intermediate versus deep dermal burns at 1 hour or 24 hours, $p = 0.95$ and $p = 0.41$, respectively.

[00105] **Deep Dermal (DD) versus Full-Thickness (FT).** Deep dermal versus full-thickness injury perfusion measurements were statistically different at 1 hour for the following parameters: deoxyHb, ($p<0.001$); tHb, ($p<0.001$); and StO_2, ($p<0.05$). oxyHb was not significant at 1 hour ($p=0.09$). At 24, 48, and 72-hour time points, all parameters remained statistically significant, with the exception of saturation.

[00106] **Intermediate Dermal (ID) versus Full-Thickness (FT).** Intermediate dermal versus full-thickness burns were statistically different for the following parameters at 1 hour: deoxyHb, $p<0.001$; tHb, $p<0.001$; and StO_2, $p<0.001$. OxyHb was not statistically significant at 1 hour, with $p=0.14$. As for all other comparisons, oxygen saturation was only significant at 1 hour and 72 hours, while all other parameters remained significant for the rest of the time points: 24, 48, and 72 hours.

Early Prediction of Burn Depth

[00107] When 1-hour tissue oxygen saturation was related to final 72 hour burn depth, there was a strong non-linear correlation ($R^2 = 0.99$) between StO_2 and burn depth. This suggested that early 1 hour tissue oxygen saturation may be related to final burn depth three days later (**FIG. 11**).

Perfusion Profiles

[00108] Intermediate dermal (ID) burn group exhibited the greatest increase in oxyHb, deoxyHb, and tHb throughout the study, followed by DD burns, which also demonstrated an increase in perfusion parameters, albeit to a lesser degree. FT burns exhibited a decrease in perfusion parameters (**FIGs. 7-9**). As part of the dermis is destroyed, an inflammatory reaction takes place, which signals for increased perfusion to the burn site. The more superficial the burn, the more of the dermal microvasculature is intact, and thus an increased demand in perfusion can be met with an increased supply and delivery to tissues. In deeper burns, where more of the dermal microvasculature is destroyed, perfusion is compromised.

[00109] Another finding in FT injury was increased oxyHb to 1.49 over baseline at 1 hour, before its drop at 24 hours. Possible explanations include the formation of traumatic microhemorrhages due to extreme thermal damage, poor oxygen extraction by the severely injured tissue, or, a combination of both.

Oxygenation Profiles

[00110] An interesting finding that did not follow prior NIR results was tissue oxygenation at 1-hour post injury. (Sowa, *et al.* **2001** *Burns* 27(3):241-249; Cross, *et al.* **2007** *Wound Repair and Regeneration* 15(3):332-340.) FT burns exhibited the greatest increase in StO_2, 2.08 fold over baseline; DD burns exhibited a 1.74 fold increase and ID burns, the smallest increase over baseline: 1.44 (**FIG. 10**). This observation may be due acute changes in vascular permeability after injury with vessels sustaining more damage and exhibiting greater vascular leak

Differentiating Burn Depth

[00111] It was found that the best predictive differentiators of burn depth at the majority of time points were tHb and deoxyHb, with the trend being: greatest rise in perfusion signifies more superficial injury. OxyHb was quite variable and did not reliably differentiate burn depths until 48 hours. StO_2 was statistically significant at 1 hour between all the burn depths, but this difference disappeared at 24 and 48 hours, suggesting oxygen saturation change at the depth measured with vsHSI, is transient. This early change in oxygen saturation is highly correlated to final burn depth and may be a predictive indicator of burn severity.

[00112] In this specification and the appended claims, the singular forms "a," "an," and "the" include plural reference, unless the context clearly dictates otherwise.

[00113] Unless defined otherwise, all technical and scientific terms used herein have the same meaning as commonly understood by one of ordinary skill in the art. Although any methods and

materials similar or equivalent to those described herein can also be used in the practice or testing of the present disclosure, the preferred methods and materials are now described. Methods recited herein may be carried out in any order that is logically possible, in addition to a particular order disclosed.

Incorporation by Reference

[00114] References and citations to other documents, such as patents, patent applications, patent publications, journals, books, papers, web contents, have been made in this disclosure. All such documents are hereby incorporated herein by reference in their entirety for all purposes. Any material, or portion thereof, that is said to be incorporated by reference herein, but which conflicts with existing definitions, statements, or other disclosure material explicitly set forth herein is only incorporated to the extent that no conflict arises between that incorporated material and the present disclosure material. In the event of a conflict, the conflict is to be resolved in favor of the present disclosure as the preferred disclosure.

Equivalents

[00115] The representative examples are intended to help illustrate the invention, and are not intended to, nor should they be construed to, limit the scope of the invention. Indeed, various modifications of the invention and many further embodiments thereof, in addition to those shown and described herein, will become apparent to those skilled in the art from the full contents of this document, including the examples and the references to the scientific and patent literature included herein. The examples contain important additional information, exemplification and guidance that can be adapted to the practice of this invention in its various embodiments and equivalents thereof.

What is claimed is:

CLAIMS

1. A method for predicting a maximal depth of thermal burn injury formation in superficial tissue of a subject, comprising:

acquiring photographic imagery of one or more areas of superficial tissue of the subject at one or more wavelengths of light and one or more time points; and

characterizing the obtained photographic imagery to measure one or more physiological properties in the one or more areas of superficial tissue to predict the maximal depth of burn injury formation in superficial tissue of the subject.

2. The method of Claim 1, wherein the one or more physiological properties are selected from tissue oxygenation and perfusion levels after exposure to thermal injury.

3. The method of Claim 1 or 2, wherein the one or more wavelengths of light are selected from the range from about 350 nm to 1,200 nm.

4. The method of any of Claims 1-3, wherein the photographic imagery is obtained within from about 1 hour to about 48 hours after a thermal exposure to predict the maximum burn depth.

5. The method of any of Claims 1-4, wherein measuring one or more physiological properties comprises detecting and quantifying the level of oxygenated hemoglobin and an increase or decrease in measured levels of oxygenated hemoglobin in the burned area of the subject is used as a biomarker to predict maximum burn depth.

6. The method of any of Claims 1-4, wherein measuring one or more physiological properties comprises detecting and quantifying the level of de-oxygenated hemoglobin and an increase or decrease in measured levels of de-oxygenated hemoglobin in burned area of a subject is used as a biomarker to predict maximum burn depth.

7. The method of any of Claims 1-4, wherein measuring one or more physiological properties comprises detecting and quantifying the level of tissue oxygen saturation and an increase or decrease in measured levels of tissue oxygen saturation in the burned area of a subject is used as a biomarker to indicate predict maximum burn depth.

8. The method of any of Claims 1-4, wherein measuring one or more physiological properties comprises detecting and quantifying the level of total hemoglobin and an increase or decrease in measured levels of total hemoglobin in the burned area of a subject is used as a biomarker to predict maximum burn depth.

9. The method of any of Claims 1-8, wherein characterizing the obtained photographic imagery is performed in conjunction with assessment of one or more of the following: collagen, lipids, water, melanin, or other naturally occurring molecules.

10. The method of any of Claims 1-9, further comprising:

characterizing the obtained photographic imagery to measure one or more physiological properties in the one or more areas of superficial tissue to estimate total body surface area of a patient's burned skin.

11. A biomedical imaging method for predicting acute skin reactions after exposure to ionizing radiation, comprising:

acquiring photographic imagery of one or more areas of superficial tissue of the subject at one or more wavelengths of light and one or more time points; and

characterizing the obtained photographic imagery to detect changes in tissue oxygenation and perfusion levels of the subject to predict acute skin reactions.

12. The method of Claim 11, wherein the acute skin reactions are selected from the group consisting of erythema, moist or dry desquamation and ulceration.

13. The method of Claim 11 or 12, wherein the one or more wavelengths of light are selected from the range from about 350 nm to 1,200 nm.

14. The method of any of Claims 11-13, wherein the photographic imagery is obtained within about 1 to about 5 days after exposure to ionizing radiation to predict acute skin reaction occurring within 1 to about 2 months.

15. The method of any of Claims 11-14, wherein measuring one or more physiological properties comprises detecting and quantifying oxygenated hemoglobin levels and an increase or decrease in measured levels of oxygenated hemoglobin in the exposed area of a subject is used as a biomarker to predict acute skin reaction.

16. The method of any of Claims 11-14, wherein measuring one or more physiological properties comprises detecting and quantifying de-oxygenated hemoglobin levels and an increase or decrease in measured levels of de-oxygenated hemoglobin in the exposed area of a subject is used as a biomarker to predict acute skin reaction.

17. The method of any of Claims 11-14, wherein one or more physiological properties comprises detecting and quantifying the level of tissue oxygen saturation and an increase or decrease in measured levels of tissue oxygen saturation in the burned area of a subject is used as a biomarker to indicate predict acute skin reaction.

18. The method of any of Claims 11-14, wherein one or more physiological properties comprises detecting and quantifying the level of total hemoglobin and an increase or

decrease in measured levels of total hemoglobin in the burned area of a subject is used as a biomarker to predict acute skin reaction.

19. The method of any of Claims 11-18, wherein characterizing the obtained photographic imagery is performed in conjunction with assessment of one or more of the following: collagen, lipids, water, melanin, or other naturally occurring molecules.

20. A biomedical imaging method for predicting acute skin reactions after exposure to thermal injury, comprising:

acquiring photographic imagery of one or more areas of superficial tissue of the subject at one or more wavelengths of light and one or more time points; and

characterizing the obtained photographic imagery to detect changes in tissue oxygenation and perfusion levels of the subject to predict acute skin reactions.

21. The method of Claim 20, wherein the acute skin reactions are selected from the group consisting of erythema, moist or dry desquamation, or ulceration.

22. The method of Claim 20 or 21, wherein the one or more wavelengths of light are selected from the range from about 350 nm to 1,200 nm.

23. The method of any of Claims 20-22, wherein the photographic imagery is obtained within from about 1 hour to about 48 hours after a thermal exposure.

24. The method of any of Claims 20-23, wherein the photographic imagery is obtained within about 3 to 5 days after exposure to thermal injury to predict acute skin reaction occurring within one month.

25. The method of any of Claims 20-24, wherein measuring one or more physiological properties comprises detecting and quantifying oxygenated hemoglobin levels and an increase or decrease in measured levels of oxygenated hemoglobin in the exposed area of a subject is used as a biomarker to predict acute skin reaction.

26. The method of any of Claims 20-24, wherein measuring one or more physiological properties comprises detecting and quantifying de-oxygenated hemoglobin levels and an increase or decrease in measured levels of de-oxygenated hemoglobin in the exposed area of a subject is used as a biomarker to predict acute skin reaction.

27. The method of any of Claims 20-24, wherein one or more physiological properties comprises detecting and quantifying the level of tissue oxygen saturation and an increase or decrease in measured levels of tissue oxygen saturation in the burned area of a subject is used as a biomarker to indicate predict acute skin reaction.

28. The method of any of Claims 20-24, wherein one or more physiological properties comprises detecting and quantifying the level of total hemoglobin and an increase or

decrease in measured levels of total hemoglobin in the burned area of a subject is used as a biomarker to predict acute skin reaction.

29. The method of any of Claims 20-28, wherein characterizing the obtained photographic imagery is performed in conjunction with assessment of one or more of the following: collagen, lipids, water, melanin, or other naturally occurring molecules.

30. The method of any of Claims 1-29, wherein the subject is a human.

31. The method of any of Claims 1-29, wherein the subject is an animal.

32. The method of any of Claims 1-29, wherein a computer algorithm for image processing is used in characterizing the obtained photographic imagery.

33. The method of any of Claims 1-29, further comprising

determining course of medical treatment or segregation of individual subjects into groups for triage in a mass casualty scenario.

34. The method of Claim 33, further comprising

segregating individual subjects into groups for triage in a mass casualty scenario.

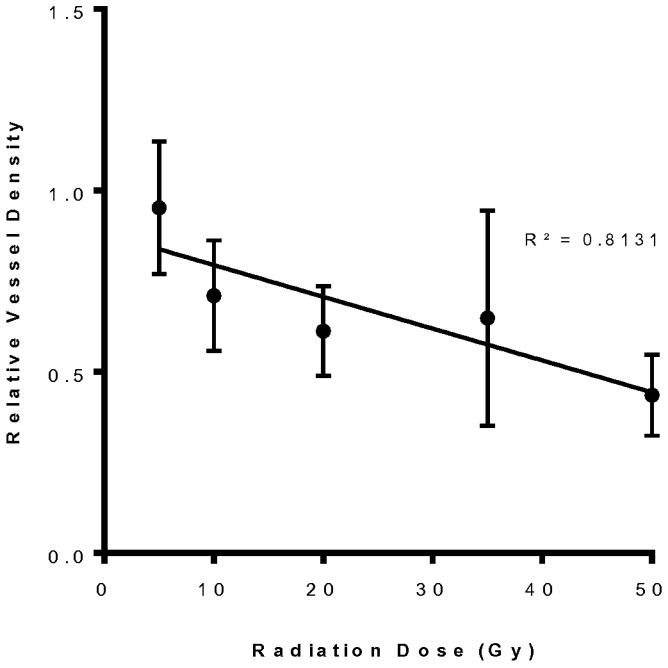
1.5
1.0
0.5
0.0
Relative Vessel Density
R² = 0.8131
0
10
20
30
40
50
Radiation Dose (Gy)

FIG. 1

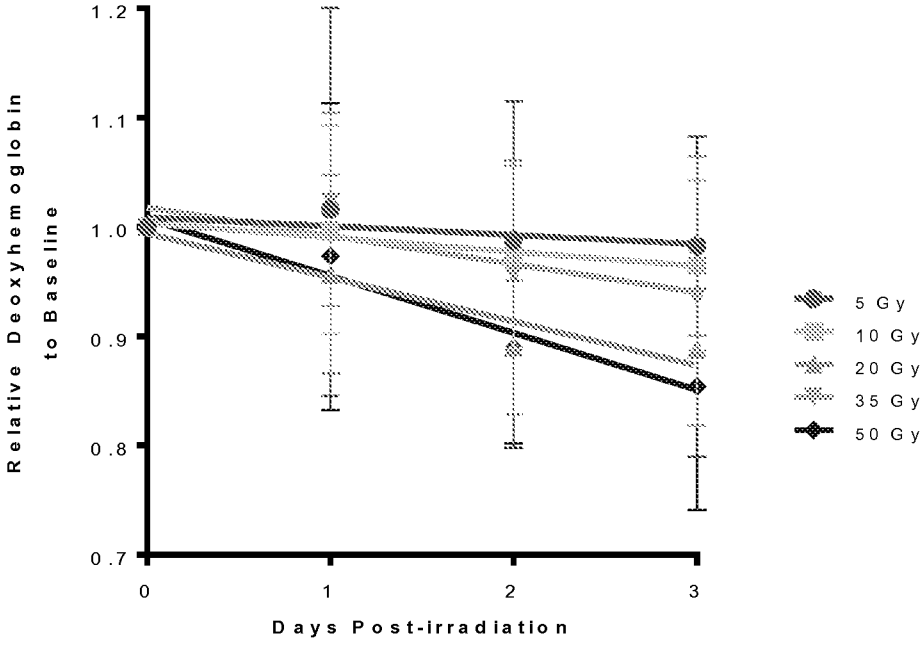
1.2
1.1
1.0
0.9
0.8
0.7
Relative Deoxyhemoglobin to Baseline
0
1
2
3
Days Post-irradiation
5 Gy
10 Gy
20 Gy
35 Gy
50 Gy

FIG. 2

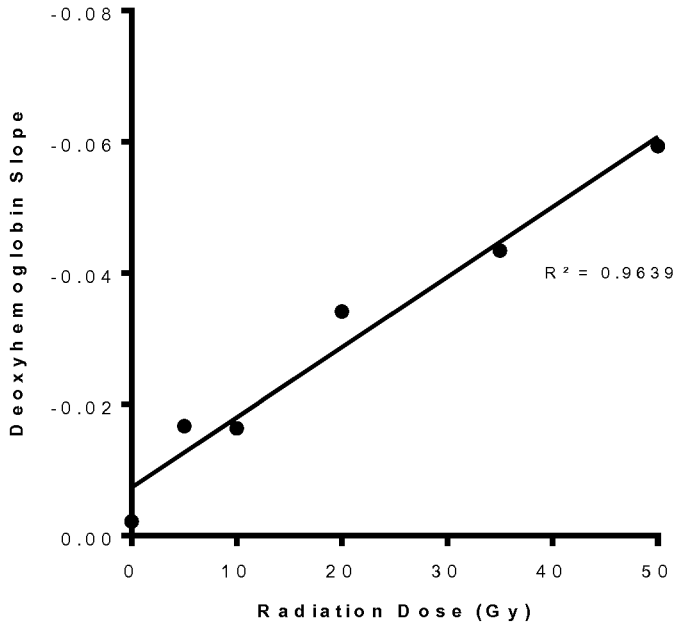
-0.08
-0.06
-0.04
-0.02
0.00
Deoxyhemoglobin Slope
R² = 0.9639
0
10
20
30
40
50
Radiation Dose (Gy)

FIG. 3

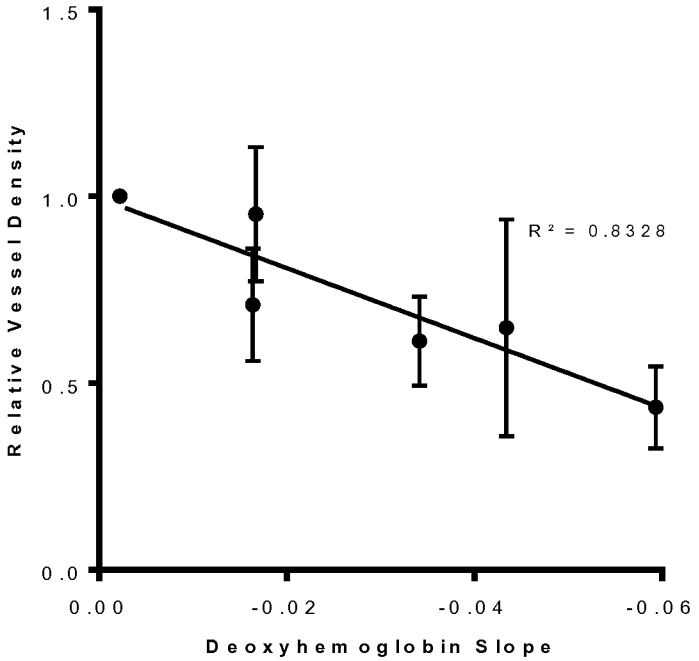
1.5
1.0
0.5
0.0
Relative Vessel Density
R² = 0.8328
0.00
-0.02
-0.04
-0.06
Deoxyhemoglobin Slope

FIG. 4

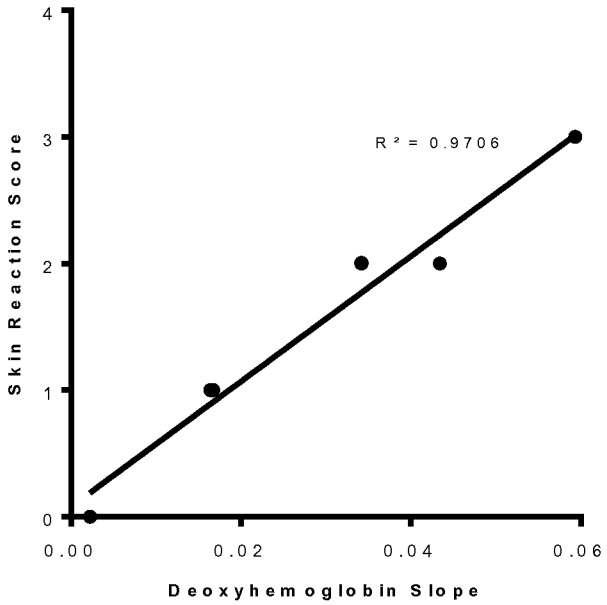
Skin Reaction Score
Deoxyhemoglobin Slope
R² = 0.9706
0
1
2
3
4
0.00
0.02
0.04
0.06

FIG. 5

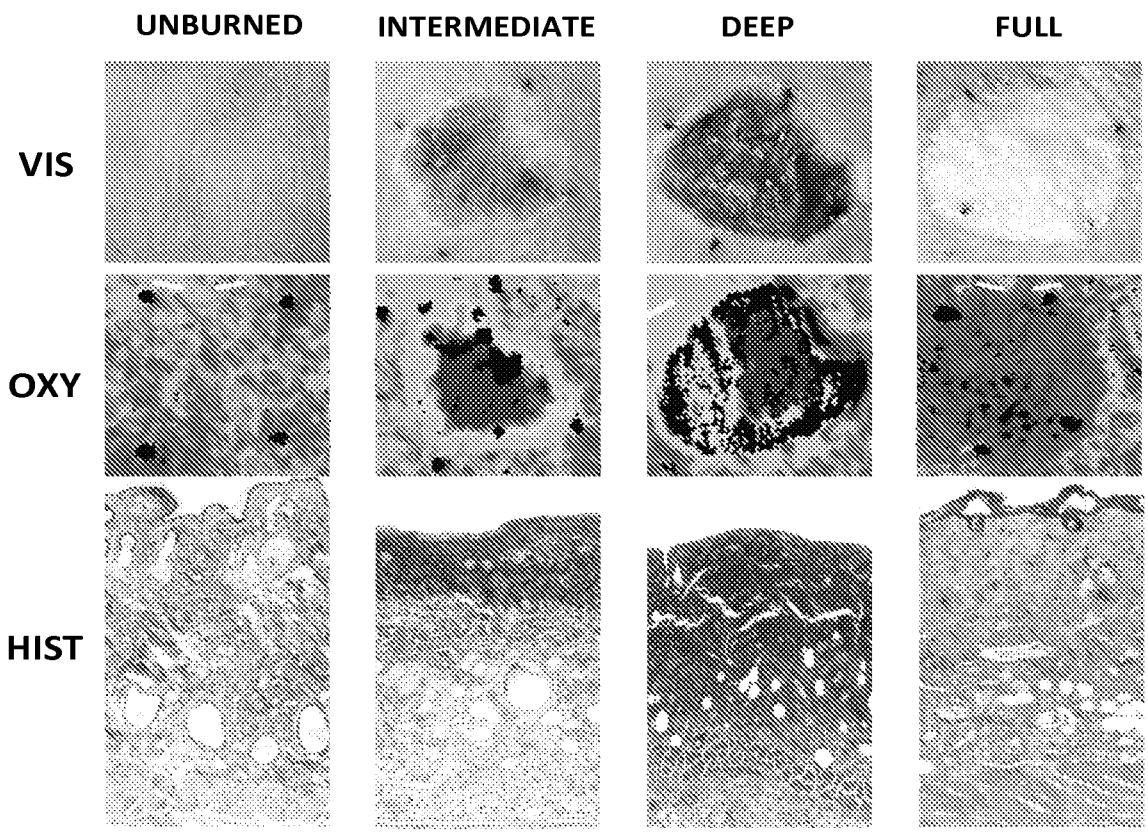
UNBURNED
INTERMEDIATE
DEEP
FULL
VIS
OXY
HIST

FIG. 6

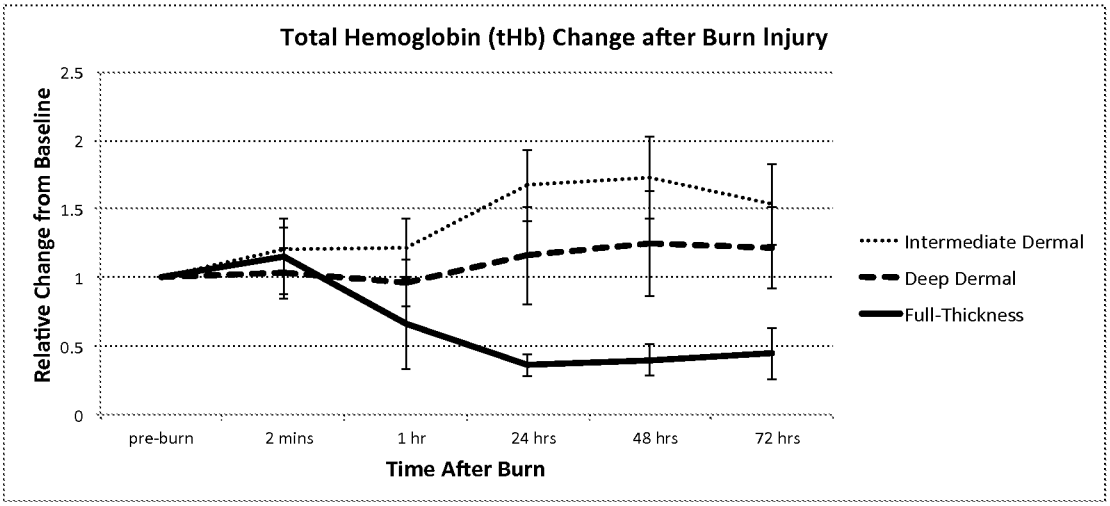

FIG. 7

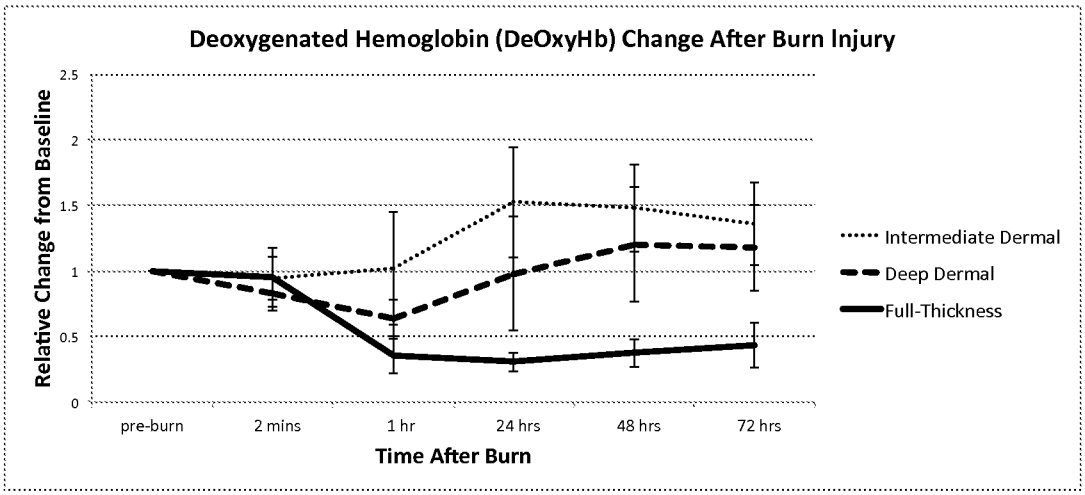

FIG. 8

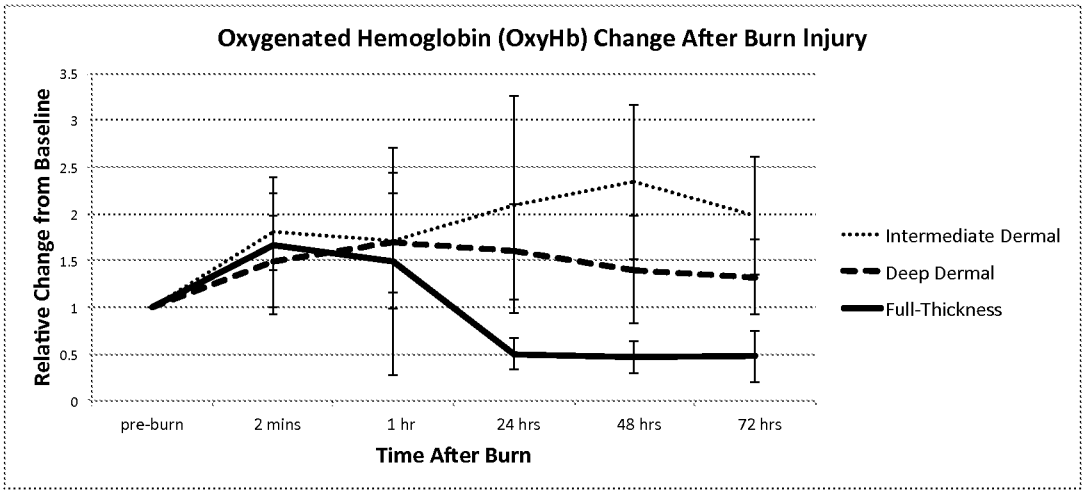

FIG. 9

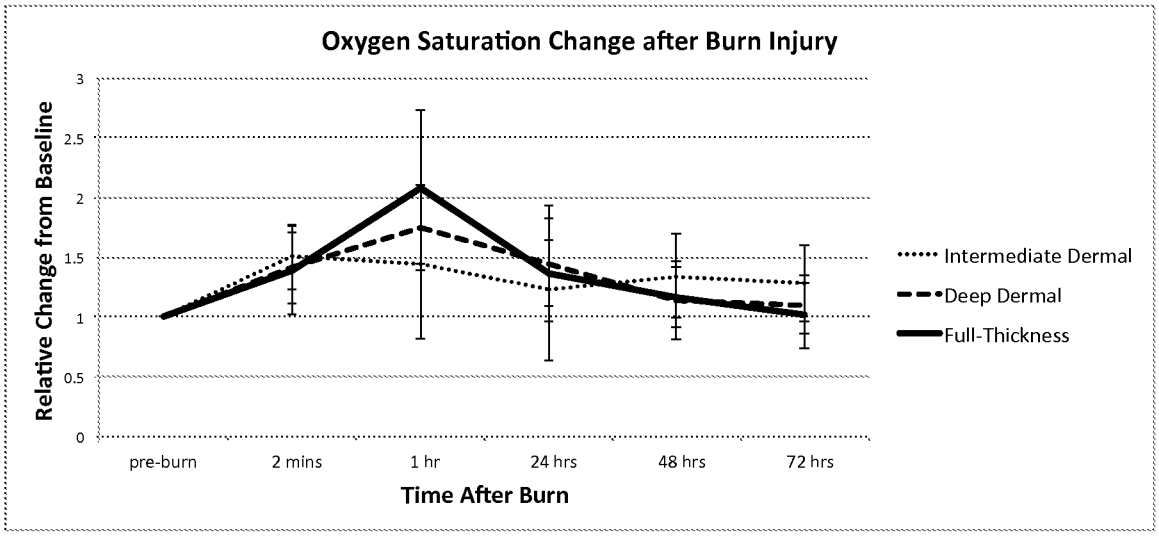
Oxygen Saturation Change after Burn Injury
Relative Change from Baseline
3
2.5
2
1.5
1
0.5
0
pre-burn
2 mins
1 hr
24 hrs
48 hrs
72 hrs
Time After Burn
Intermediate Dermal
Deep Dermal
Full-Thickness

FIG. 10

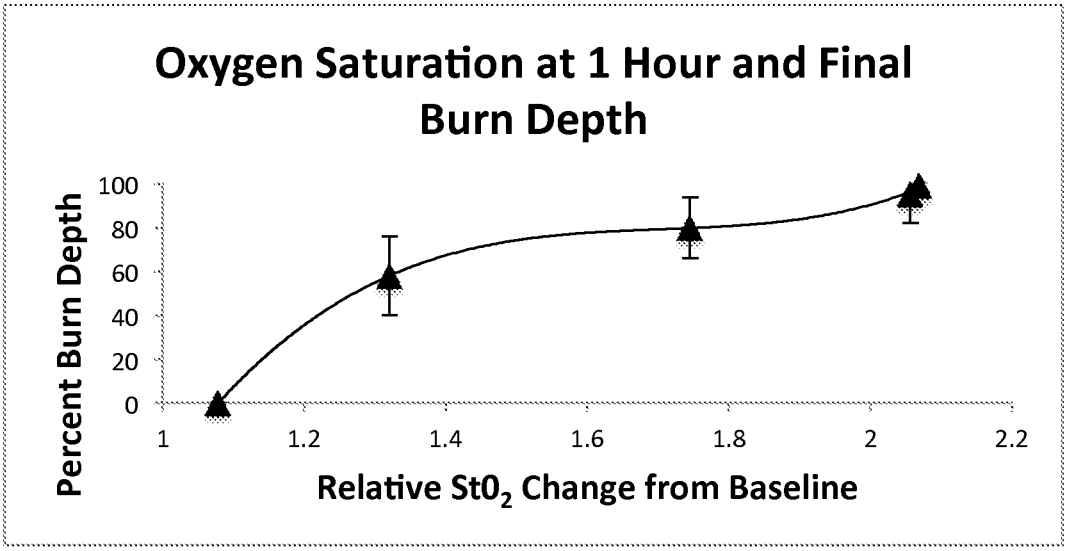
Oxygen Saturation at 1 Hour and Final Burn Depth
Percent Burn Depth
100
80
60
40
20
0
1
1.2
1.4
1.6
1.8
2
2.2
Relative St0$_2$ Change from Baseline

FIG. 11

INTERNATIONAL SEARCH REPORT

International application No.
PCT/US 15/33229

A. CLASSIFICATION OF SUBJECT MATTER
IPC(8) - A61B 5/00 (2015.01)
CPC - G06T 2207/30088, G06T 7/0012, A61B 5/443, A61B 5/4869
According to International Patent Classification (IPC) or to both national classification and IPC

B. FIELDS SEARCHED

Minimum documentation searched (classification system followed by classification symbols)
IPC(8) - A61B 5/00 (2015.01)
CPC - G06T 2207/30088, G06T 7/0012, A61B 5/443, A61B 5/4869

Documentation searched other than minimum documentation to the extent that such documents are included in the fields searched
USPC: 382/128, 130, 133, 600/310-344, 473-480; CPC: G06T 7/0014, 7/0016; G06T 2207/30004-2207/30104; A61B 5/0059-5/0091; A61B 5/0261; A61B 5/441-5/447 (Search term limited; see below)

Electronic data base consulted during the international search (name of data base and, where practicable, search terms used)
PubWest (PGPB, USPT, EPAB, JPAB); Google; PatBase (All);
Search Terms: Thermal, heat, burn, radiation, xray, ioniz*, gamma, injury, damage, exposure, predict*, diagnos*, skin, tissue, epiderm*, derm*, subderm*, skin reaction, erythema, desquam*, ulcer*, perfusion, oxygen*, hemoglobin, blood, concentration, amount, quantity

C. DOCUMENTS CONSIDERED TO BE RELEVANT

Category*	Citation of document, with indication, where appropriate, of the relevant passages	Relevant to claim No.
X	US 2006/0155193 A1 (LEONARDI et al.) 13 July 2006 (13.07.2006) Entire document, especially Abstract, para[0009]- para[0010], para[0026]- para[0030], para[0040] and FIGS. 3-4.	1, 2, 3/(1-2)
X	WO 2013/082192 A1 (CHIN) 06 June 2013 (06.06.2013) Entire document, especially Abstract, para[0014]- para[0017], para[0039]- para[0046].	11, 12-13/(11/2), 20, 21, 22/(20-21)
A	US 2004/0039379 A1 (VIATOR et al.) 26 February 2004 (26.02.2004) Entire document.	1-3, 11-13, 20-22
A	US 5,810,010 A (ANBAR) 22 September 1998 (22.09.1998) Entire document.	1-3, 11-13, 20-22
A	WO 2013/162358 A1 (GOETHALS) 31 October 2013 (31.10.2013) Entire document.	1-3, 11-13, 20-22
A	US 2007/0012886 A1 (TEARNEY et al.) 18 January 2007 (18.01.2007) Entire document.	1-3, 11-13, 20-22

☐ Further documents are listed in the continuation of Box C. ☐

* Special categories of cited documents:
"A" document defining the general state of the art which is not considered to be of particular relevance
"E" earlier application or patent but published on or after the international filing date
"L" document which may throw doubts on priority claim(s) or which is cited to establish the publication date of another citation or other special reason (as specified)
"O" document referring to an oral disclosure, use, exhibition or other means
"P" document published prior to the international filing date but later than the priority date claimed
"T" later document published after the international filing date or priority date and not in conflict with the application but cited to understand the principle or theory underlying the invention
"X" document of particular relevance; the claimed invention cannot be considered novel or cannot be considered to involve an inventive step when the document is taken alone
"Y" document of particular relevance; the claimed invention cannot be considered to involve an inventive step when the document is combined with one or more other such documents, such combination being obvious to a person skilled in the art
"&" document member of the same patent family

Date of the actual completion of the international search	Date of mailing of the international search report
18 August 2015 (18.08.2015)	04 SEP 2015
Name and mailing address of the ISA/US Mail Stop PCT, Attn: ISA/US, Commissioner for Patents P.O. Box 1450, Alexandria, Virginia 22313-1450 Facsimile No. 571-273-8300	Authorized officer: Lee W. Young PCT Helpdesk: 571-272-4300 PCT OSP: 571-272-7774

Form PCT/ISA/210 (second sheet) (January 2015)

INTERNATIONAL SEARCH REPORT

International application No.
PCT/US 15/33229

Box No. II Observations where certain claims were found unsearchable (Continuation of item 2 of first sheet)

This international search report has not been established in respect of certain claims under Article 17(2)(a) for the following reasons:

1. ☐ Claims Nos.:
because they relate to subject matter not required to be searched by this Authority, namely:

2. ☐ Claims Nos.:
because they relate to parts of the international application that do not comply with the prescribed requirements to such an extent that no meaningful international search can be carried out, specifically:

3. ☒ Claims Nos.: 4-10, 14-19, 23-34
because they are dependent claims and are not drafted in accordance with the second and third sentences of Rule 6.4(a).

Box No. III Observations where unity of invention is lacking (Continuation of item 3 of first sheet)

This International Searching Authority found multiple inventions in this international application, as follows:

1. ☐ As all required additional search fees were timely paid by the applicant, this international search report covers all searchable claims.

2. ☐ As all searchable claims could be searched without effort justifying additional fees, this Authority did not invite payment of additional fees.

3. ☐ As only some of the required additional search fees were timely paid by the applicant, this international search report covers only those claims for which fees were paid, specifically claims Nos.:

4. ☐ No required additional search fees were timely paid by the applicant. Consequently, this international search report is restricted to the invention first mentioned in the claims; it is covered by claims Nos.:

Remark on Protest

☐ The additional search fees were accompanied by the applicant's protest and, where applicable, the payment of a protest fee.

☐ The additional search fees were accompanied by the applicant's protest but the applicable protest fee was not paid within the time limit specified in the invitation.

☐ No protest accompanied the payment of additional search fees.

专利名称(译)	高光谱成像用于预测暴露于热能或电离辐射后的皮肤损伤		
公开(公告)号	EP3151735A1	公开(公告)日	2017-04-12
申请号	EP2015803959	申请日	2015-05-29
申请(专利权)人(译)	马萨诸塞州大学医学院		
当前申请(专利权)人(译)	马萨诸塞州大学医学院		
[标]发明人	CHIN MICHAEL S		
发明人	CHIN, MICHAEL S.		
IPC分类号	A61B5/00		
CPC分类号	A61B5/7275 A61B5/0075 A61B5/14551 A61B5/443 A61B5/445 A61B2576/00 G16H30/40 G16H50/20		
优先权	62/007891 2014-06-04 US		
其他公开文献	EP3151735A4		
外部链接	Espacenet		

摘要(译)

本发明提供了基于高光谱成像的方法，其能够有效，有效和无创地检测和表征组织中的热和电离辐射。该方法允许完全可视化和量化热烧伤或电离辐射影响皮肤中的氧合和灌注变化，并且能够快速识别暴露于这种暴露的个体，并且允许在暴露后早期预测正常组织中的损伤程度。